Optimal driving strategies for traffic control with autonomous vehicles

Thibault Liard [*] **Raphael Stern** [**]
Maria Laura Delle Monache [***]

[*] *Chair of Computational Mathematics, Fundación Deusto, Av. de las Universidades 24, 48007 Bilbao, Basque Country, Spain (e-mail: thibault.liard@deusto.es)*
[**] *Department of Civil, Environmental, and Geo- Engineering, University of Minnesota, USA (e-mail: rstern@umn.edu)*
[***] *Univ. Grenoble Alpes, Inria, CNRS, Grenoble INP, GIPSA-Lab, 38000 Grenoble, France, (e-mail: ml.dellemonache@inria.fr)*

Abstract:
This article considers the possibility of using a small number of autonomous vehicles (AV) for traffic control of the predominantly human-piloted traffic. Specifically, we consider the control of the AV to act as a moving bottleneck, which will be used to optimize traffic flow properties such as fuel consumption of the combined human-piloted and autonomous traffic flow.
We use a coupled partial differential equation (PDE)-ordinary differential equation (ODE) framework to model the bulk traffic flow using a PDE, and the trajectory of an autonomous vehicle in the flow using an ODE, depending on the downstream traffic density. The autonomous vehicle acts on the traffic flow as a moving bottleneck via a moving flux constraint. Using this modeling framework, we consider an optimal control problem which consists in finding the optimal AV trajectory to minimize fuel consumption of the entire traffic flow. We prove existence of optimal AV trajectories and we present two different optimal driving strategies depending on the initial traffic conditions.

Keywords: Autonomous vehicles, Traffic control systems, Intelligent transportation systems, Control of partial differential equations, Modeling for control optimization

1. INTRODUCTION

Moving bottlenecks on roadways such as slower moving vehicles or large trucks that drive slower than the remaining traffic are often considered to be obstacles that disrupt the flow of traffic. However, recently, the notion of using moving bottlenecks as control agents in the traffic flow has been proposed (e.g., Ramadan and Seibold (2017); Čičić and Johansson (2018); Piacentini et al. (2018)). The idea being that a moving bottleneck might locally disrupt the traffic flow, but could be used to control the flow of traffic and optimize a global traffic property such as fuel consumption. Wihh autonomous vehicle (AV) technology rapidly advancing and the promise of a small number of AVs soon being deployed, it is possible that these AVs could be used as moving bottlenecks to locally control the flow of traffic and reduce fuel consumption of the entire traffic stream.

The use of AVs for traffic control in the flow has previously been explored experimentally by Stern et al. (2018), who showed that AVs, with a penetration rate as low as 5%, were capable of stabilizing the traffic flow and substantially reducing the fuel consumption of the entire traffic stream. However, this work did not consider vehicle overtaking, and thus, the AV acted more as a pace vehicle than a bottleneck.

The use of AVs as a moving bottleneck for traffic control has been explored by Piacentini et al. (2018) and Čičić and Johansson (2018). Here the AV speed profile is adjusted based on the local density. Such analysis is enabled by the coupled ordinary differential equation (ODE) and partial differential equation (PDE) modeling framework introduced by Delle Monache and Goatin (2014). This model describes the bulk traffic flow using fluid mechanics models via a PDE, which is coupled with the individual vehicle dynamics of the moving bottleneck described by an ODE.

In this work, we consider the control of a single AV in the flow of human driven traffic and use the AV as a moving bottleneck to control the traffic flow and reduce the overall vehicle fuel consumption of the entire traffic stream using different initial traffic conditions. In comparison to prior work by Piacentini et al. (2018), the vehicle speed is changed at optimal intervals instead of at specific points in time, while Čičić and Johansson (2018) use a different vehicle flux function for the bulk traffic flow, which influences the dynamics of the moving bottleneck. Moreover, in our work, the moving bottleneck is allowed to slow down to zero speed and become a fixed bottleneck if it is advantageous from a fuel consumption standpoint. This is considered for both constant and non-constant initial traffic density conditions. Furthermore, while the results by Piacentini et al. (2018) use model predictive control

leading to a non-optimal control strategy. In contrast, the results presented in this paper seems to be optimal with respect to fuel consumption.

The remainder of this article is outlined as follows. In Section 2, the coupled PDE-ODE model is introduced, and the corresponding Riemann and Cauchy problems are presented. In Section 3 the numerical solver for the PDE and for the ODE are described, and in Section 4 the control problem to minimize total fuel consumption via speed control of the AV as a moving bottleneck is presented. The results from numerical experiments are in Section 5, which show that the AV is able to reduce fuel consumption of the entire traffic stream if properly controlled as a moving bottleneck. Finally, we conclude in Section 6.

2. DESCRIPTION OF THE MODEL

We briefly outline the coupled PDE-ODE model used to describe both the macroscopic traffic flow as well as the dynamics of the moving bottleneck.

Let the constants $\rho_{\max}$ and $V_{\max}$ be respectively the maximum density and the maximum road speed. We denote by BV, the set of functions of bounded variation. We study a strongly coupled PDE-ODE system described by

$$\partial_t \rho(t,x) + \partial_x f(\rho(t,x)) = 0, \quad t>0,\, x\in\mathbb{R}, \tag{1a}$$
$$\dot{y}(t) = \min\{V_d(t), v(\rho(t,y(t)+))\}, \quad t>0, \tag{1b}$$
$$f(\rho(t,y(t))) - \dot{y}(t)\rho(t,y(t)) \le F_\alpha(\dot{y}(t)), \quad t>0, \tag{1c}$$
$$\rho(0,x) = \rho_0(x), \quad x\in\mathbb{R}, \tag{1d}$$
$$y(0) = y^0, \tag{1e}$$

where $\rho = \rho(t,x) \in [0,\rho_{\max}]$ denotes the macroscopic traffic density at time $t \ge 0$ and at position $x \in \mathbb{R}$, the flux function f is defined by

$$f(\rho) = \rho v(\rho),$$

where v is the mean speed of cars, $y(\cdot)$ stands for the trajectory of the AV, $V_d \in BV(\mathbb{R}_+,[0,V_{\max}])$ is the maximum speed of the AV, $\alpha \in (0,1)$ and $F_\alpha(\dot{y}(t)) := \frac{\alpha\rho_{\max}}{4V_{\max}}(\dot{y}(t)-V_{\max})^2$.

The model (1) was first introduced by Delle Monache and Goatin (2014) and models the impact of an AV on the evolution of the traffic flow. Above, The PDE (1a) is the macroscopic model named LWR model (see Richards (1956); Lighthill and Whitham (1955)). We assume that the speed v depends linearly on the density of cars as follows:

$$v(\rho) = V_{\max}\left(1-\frac{\rho}{\rho_{\max}}\right). \tag{2}$$

The trajectory of the autonomous vehicle is modeled by an ODE described in (1b). The autonomous vehicle drives at its desired speed except when the surrounding traffic is too dense. In this case, the autonomous vehicle reduce its velocity accordingly. The autonomous vehicle influences indirectly the evolution of the traffic flow via the moving flux constraint (1c).

We fix the following notation: let $V \to \check{\rho}_\alpha(V)$ and $V \to \hat{\rho}_\alpha(V)$ such that $\check{\rho}_\alpha(V) < \hat{\rho}_\alpha(V)$ be the two solutions of $F_\alpha(V) + V\rho = f(\rho)$ and let ρ^* the solution of $V\rho = f(\rho)$ (see Figure 1). We compute $V \to \check{\rho}_\alpha(V)$, $V \to \hat{\rho}_\alpha(V)$ and $V \to \rho^*$ using the fact that f is strictly concave and $v(\rho) = V_{\max}\left(1-\frac{\rho}{\rho_{\max}}\right)$. For every $V \in [0,V_{\max}]$, we obtain:

$$\check{\rho}_\alpha(V) = \rho_{\max}(V_{\max}-V)\left(\frac{1-\sqrt{1-\alpha}}{2V_{\max}}\right), \tag{3}$$
$$\hat{\rho}_\alpha(V) = \rho_{\max}(V_{\max}-V)\left(\frac{1+\sqrt{1-\alpha}}{2V_{\max}}\right), \tag{4}$$
$$\rho^*(V) = \rho_{\max}\left(1-\frac{V}{V_{\max}}\right). \tag{5}$$

Moreover, we denote by $\sigma(\rho_1,\rho_2) := \frac{f(\rho_1)-f(\rho_2)}{\rho_1-\rho_2}$ the

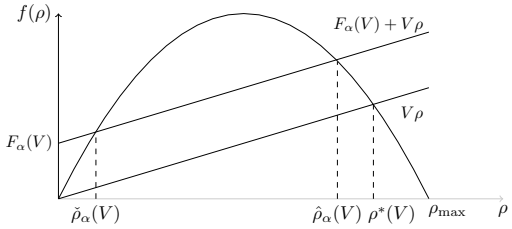

Fig. 1. The flux function f and $\check{\rho}_\alpha(V) \leqslant \hat{\rho}_\alpha(V) \leqslant \rho^*(V)$.

Rankine-Hugoniot speed of the front wave (ρ_1,ρ_2).

2.1 The Riemann problem with moving constraints

We consider (1) with Riemann type initial data

$$\rho_0(x) = \begin{cases} \rho_L \text{ if } & x<0 \\ \rho_R \text{ if } & x>0 \end{cases} \quad \text{and} \quad y_0 = 0. \tag{6}$$

The definition of the constrained Riemann solver for (1) and (6) is described in (Delle Monache and Goatin, 2014, Section 3) and Garavello et al. (2019). We denote by $\mathcal{R}$ the standard Riemann solver for (1a) and (1d) where ρ_0 is defined in (6).

Definition 1. Let $V \in [0,V_{\max}]$. The constrained Riemann solver $\mathcal{R}^V : [0,\rho_{\max}]^2 \mapsto L^1_{\text{loc}}(\mathbb{R};[0,\rho_{\max}])$ for (1) and (6) is defined as follows:

(1) If $f(\mathcal{R}(\rho_L,\rho_R)(V)) > F_\alpha(V) + V\mathcal{R}(\rho_L,\rho_R)(V)$, then
$$\mathcal{R}^V(\rho_L,\rho_R)(x/t) = \begin{cases} \mathcal{R}(\rho_L,\hat{\rho}_\alpha(V))(x/t) \text{ if } & x<Vt, \\ \mathcal{R}(\check{\rho}_\alpha(V),\rho_R)(x/t) \text{ if } & x\geqslant Vt, \end{cases}$$
and $y(t) = V$.

(2) If $V\mathcal{R}(\rho_L,\rho_R)(V) \leqslant f(\mathcal{R}(\rho_L,\rho_R)(V)) \leqslant F_\alpha(V) + V\mathcal{R}(\rho_L,\rho_R)(V)$, then
$$\mathcal{R}^V(\rho_L,\rho_R) = \mathcal{R}(\rho_L,\rho_R) \quad \text{and} \quad y(t) = V.$$

(3) If $f(\mathcal{R}(\rho_L,\rho_R)(V)) < V\mathcal{R}(\rho_L,\rho_R)(V)$, then
$$\mathcal{R}^V(\rho_L,\rho_R) = \mathcal{R}(\rho_L,\rho_R) \quad \text{and} \quad y(t) = v(\rho_R)t.$$

An illustration of each case in Definition 1 is given in Figure 2, Figure 3 and Figure 4.

2.2 The Cauchy problem

Let us consider an initial position $y_0 \in \mathbb{R}$ of the AV, a desired speed $V_d \in BV\left(\mathbb{R}^+;[0,V_{\max}]\right)$ of the AV and an initial density $\rho_0 \in \left(L^1 \cap BV\right)(\mathbb{R};[0,\rho_{\max}])$

Definition 2. The couple (ρ,y) provides a solution to (1) if the following conditions hold.

(1) $\rho \in C^0\left(\mathbb{R}^+;\left(L^1\cap BV\right)(\mathbb{R};[0,\rho_{\max}])\right)$;

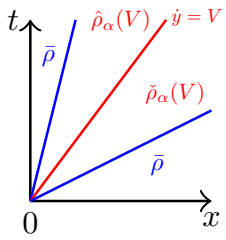

Fig. 2. The solution of the constrained Riemann problem of (1) with $\rho_L = \rho_R = \bar{\rho} \in (\check{\rho}_\alpha(V), \hat{\rho}_\alpha(V))$: case (1) of Definition 1.

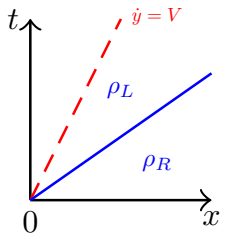

Fig. 3. The solution of the constrained Riemann problem of (1) with $0 < \rho_L < \check{\rho}_\alpha(V)$ and $\hat{\rho}_\alpha(V) < \rho_R \leqslant \rho_{\max}$: case (2) of Definition 1.

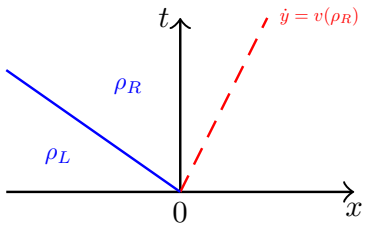

Fig. 4. The solution of the constrained Riemann problem of (1) with $\rho^*(V) < \rho_L < \rho_R$: case (3) of Definition 1.

(2) $y \in W^{1,1}_{\text{loc}}(\mathbb{R}^+;\mathbb{R})$;
(3) ρ is a weak solution of $\partial_t \rho + \partial_x f(\rho) = 0$ in $\mathbb{R}^+ \times \mathbb{R}$
(4) For every $\kappa \in \mathbb{R}$ and for all $\varphi \in C^1_c(\mathbb{R}^2;\mathbb{R}^+)$ it holds

$$\int_{\mathbb{R}^+}\int_{\mathbb{R}} \left(|\rho-\kappa|\partial_t\varphi + \text{sgn}(\rho-\kappa)g(k)\partial_x\varphi\right) dx\, dt \quad (7)$$

$$+2\int_{\mathbb{R}^+} \left(h(k) - \min\{h(k), F_\alpha(\dot{y}(t))\}\right)\varphi(t,y(t))\, dt \quad (8)$$

$$+\int_{\mathbb{R}} |\rho_0-\kappa|\varphi(0,x)\, dx \geqslant 0\,;$$

with $g(k) = f(\rho) - f(\kappa)$ and $h(k) = f(\kappa) - \dot{y}(t)\kappa$.
(5) For a.e. $t > 0$, $\dot{y}(t) = \min\{V_d(t), v(\rho(t, y(t)+))\}$;
(6) For a.e. $t > 0$, $f(\rho(t,y(t)\pm)) - \dot{y}(t)\rho(t,y(t)\pm) \leq F_\alpha(\dot{y}(t))$.

Theorem 1. (Garavello et al. (2019)) The Cauchy problem (1) admits a solution in the sense of Definition 2.

Remark 1. The main ideas to prove Theorem 1 are as follows. Fixing V_d, ρ_0 and y_0, Garavello et al. (2019) construct an approximate solution (ρ^n, y^n) of (1) using a wave-front tracking algorithm described in the next section. They prove that the couple (ρ^n, y^n) converges, as $n \to \infty$, to a solution (ρ, y) of (1) in the sense of Definition 2. In particular, we have

$$\lim_{n\to\infty} \|\rho^n(t,\cdot) - \rho(t,\cdot)\|_{L^1_{\text{loc}}(\mathbb{R})} = 0,$$

and $TV(\rho) \leqslant TV(\rho^n) \leqslant TV(\rho_0) + 2\rho_{\max} + TV(V_d)$. Above, $TV(\rho)$ stands for the total variation of ρ.

3. WAVE-FRONT TRACKING ALGORITHM

We briefly describe the solution method used to solve the coupled PDE-ODE. Let ρ_0 and y_0 be fixed, we construct a density mesh $\mathcal{M}_n$ on the interval $[0, \rho_{\max}]$ and a velocity mesh $\mathcal{V}_n$ on the interval $[0, V_{\max}]$ such that for every $V \in \mathcal{V}_n$, $(\check{\rho}_\alpha(V), \hat{\rho}_\alpha(V)) \in (\mathcal{M}_n)^2$. Moreover, we consider two sequences of piecewise constant functions $(V_n)_{n\in\mathbb{N}}$ and $(\rho_0^n)_{n\in\mathbb{N}}$ having both a finite number of discontinuities such that

$$\lim_{n\to+\infty} \|\rho_0^n - \rho_0\|_{L^1(\mathbb{R})} = 0 \qquad \text{and} \qquad TV(\rho_0^n) \leqslant TV(\rho_0), \quad (9)$$

$$\lim_{\nu\to+\infty} \|V_n - V\|_{L^1(\mathbb{R}^+)} = 0 \qquad \text{and} \qquad TV(V_n) \leqslant TV(V), \quad (10)$$

using the method described in Garavello et al. (2019).

Since we consider a scalar problem, we adapt the first algorithm proposed in Dafermos (1972). Let $(x_k^n)_{k=1,\cdots,M}$ and $(t_k^n)_{k=1,\cdots,P}$ be the $M \in \mathbb{N}$ discontinuous points of ρ_0^n and $P \in \mathbb{N}$ discontinuous points of V_d^n respectively. The algorithm proceeds as follows: At each point of discontinuity of ρ_0^n, we solve approximately the constrained Riemann problem as described in Section 2.1 over $[0, t_1^n]$ with $V = V_d(\frac{t_1^n}{2})$. By piecing solutions together, we construct a solution ρ^n until two waves meet at t_I. If $t_I < t_1^n$, the approximate solution $\rho^n(t_I, \cdot)$ is still a piecewise constant function verifying $\rho^n(t_I, x) \in \mathcal{M}_n$ for almost every $x \in \mathbb{R}$. The corresponding Riemann problems with $V = V_d(\frac{t_1^n}{2})$ can again be approximately solved over $[t_I, t_1^n)$ within the class of piecewise constant functions and so on until $t_I = t_1^n$. When $t_I = t_1^n$, the constrained Riemann problem is again solved over $[t_1^n, t_2^n]$ as previously replacing $V_d(\frac{t_1^n}{2})$ by $V_d\left(\frac{t_2^n - t_1^n}{2}\right)$ and $\rho_0^n(\cdot)$ by $\rho^n(t_1^n, \cdot)$ and so on. Let y^n the solution of

$$\begin{cases} \dot{y}(t) = \min(V_d^n(t), v(\rho^n(t, y(t)+))), & t \in [0, t_1], \\ y(0) = y_0, & x \in \mathbb{R}. \end{cases} \quad (11)$$

where $\rho^n(t,\cdot)$ corresponds to the wave-front tracking approximate solution at time $t \in [0, t_1]$ with initial data ρ_0^n.

4. AV CONTROL PROBLEM

In this section, we present a numerical example to demonstrate how an AV can be used as a moving bottleneck to control the flow of traffic and optimize the fuel consumption of the overall traffic flow. The specific scenario considered in this numerical example is explained, as well as the numerical strategy for optimizing the AV trajectory.

4.1 Fuel consumption model

The objective of the optimization is to drive the AV in such a way that it minimizes the fuel consumption of the entire traffic flow, i.e. the total fuel consumed by all vehicles. Therefore, it is important to be able to quantify the fuel

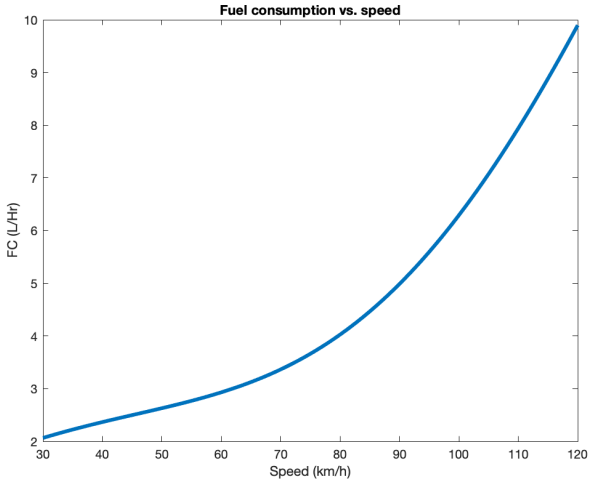

Fig. 5. Fuel consumption of a vehicle as a function of vehicle speed.

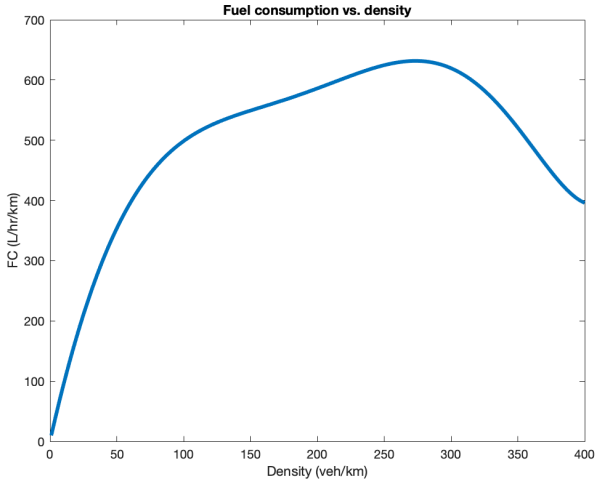

Fig. 6. Fuel consumption rate of the bulk traffic flow as a function of traffic density

consumed as a function of the vehicle density, which can be integrated over the entire roadway to calculate the total fuel consumed.

Fuel consumption is related to the speed of vehicles as shown by Ahn et al. (2002) and Berry (2010). Generally, fuel consumption increases with the speed of the vehicle, with a nonlinear relationship between speed and fuel consumption. Using the fuel consumption rates of four different commercially available vehicles, Ramadan and Seibold (2017) obtained the following best-fit model for fuel rate $K(v)$ in liters per hour (ℓ/h) as a function of speed v:

$$K(v) = 5.7\times10^{-12}v^6 - 3.6\times10^{-9}v^5 + 7.6\times10^{-7}v^4 - 6.1\times10^{-5}v^3 + 1.9\times10^{-3}v^2 + 1.6\times10^{-2}v + 0.99$$

for speed v in km/h and fuel consumption rate K in units of ℓ/h. This relationship is depicted in Figure 5.

Using the relationship between speed and fuel rate in Figure 5 as well as the relationship between density and speed in (2) obtained by assuming the LWR model, it is possible to compute the fuel rate $F(\rho)$ as a function of traffic density with units ℓ/h by computing:

$$F(\rho) = \rho K(U(\rho)), \tag{12}$$

which is depicted in Figure 6.

Let $T_f > 0$, $C > 0$ and $x_1, x_2 \in \mathbb{R}$ such that $x_1 < x_2$. We consider thus the following optimal problem

$$\inf_{\substack{V\in BV([0,T_f],[0,V_{\max}])\\ \|V\|_{BV}\leqslant C}} J(V) := \int_0^{T_f}\int_{x_1}^{x_2} F(\rho(t,x))dtdx, \tag{13}$$

with ρ the solution of (1) associated to a given initial data ρ_0. The functional J represents the Total Fuel Consumption (named TFC) computed on a highway section of length $x_2 - x_1$ km during T_f hours.

Theorem 2. The optimal problem (13) has at least one optimal solution.

PROOF. There exists a minimizing sequence $(V_m)_{m\in\mathbb{N}}$ verifying that

$$\inf_V J(V) \leqslant J(V_m) \leqslant \inf_V J(V) + \frac{1}{m}.$$

Since $V_m \in BV([0,T_f];[0,V_{\max}])$, there exists an approximate function $V_{m,n} : t \to \mathcal{V}_n$ of V_m such that

$$\lim_{n\to+\infty} \|V_{m,n} - V_m\|_{L^1([0,T_f];[0,V_{\max}])} = 0$$

and, for every $n \in \mathbb{N}$, $TV(V_{m,n}) \leqslant TV(V_m) \leqslant C$. From Remark 1, we construct an approximate solution $\rho^{m,n}$ of (1) that converges, as $n \to \infty$, to a solution (ρ^m, y^m) of (1) in the sense of Definition 2 with $V_d = V_m$. In particular, we have

$$\lim_{n\to\infty} \|\rho^{m,n}(t,\cdot) - \rho^m(t,\cdot)\|_{L^1([x_1,x_2];[0,\rho_{\max}])} = 0,$$

and there exists $C > 0$ independent of n and m such that

$$TV(\rho^m) \leqslant TV(\rho^{m,n}) \leqslant C.$$

By dominated convergence theorem,

$$\lim_{n\to\infty}\int_0^{T_f}\int_{x_1}^{x_2} F(\rho^{m,n})dtdx = \int_0^{T_f}\int_{x_1}^{x_2} F(\rho^m)dtdx. \tag{14}$$

From (14), there exists a function $\varphi : n \to \mathbb{N}$ strictly increasing such that

$$|J(V_{m,\varphi(m)}) - J(V_m)| \leqslant \frac{1}{m}. \tag{15}$$

Combining (14) and (15), we deduce that $(V_{m,\varphi(m)})_{m\in\mathbb{N}}$ is also a minimizing sequence. Helly's Theorem, see (Rudin, 1976, Theorem 7.25), implies that there exists a function $V \in BV([0,T_f];[0,V_{\max}])$ and a subsequence of $V_{m,\varphi(m)}$, still denoted by $V_{m,\varphi(m)}$, such that $V_{m,\varphi(m)}$ converges to V in $L^1([0,T_f];[0,V_{\max}])$ and $TV(V) \leqslant \liminf_m TV(V_{m,\varphi(m)}) \leqslant C$. From Remark 1, we construct an approximate solution $\rho^{m,\varphi(m)}$ of (1) associated to (V,ρ_0,y_0) that converges, as $m \to \infty$, to a solution (ρ, y) of (1) in the sense of Definition 2. Thus, we have

$$\lim_{m\to\infty} \|\rho^{m,\varphi(m)}(t,\cdot) - \rho(t,\cdot)\|_{L^1([x_1,x_2];[0,\rho_{\max}])} = 0,$$

and there exists $C > 0$ independent of m such that

$$TV(\rho) \leqslant TV(\rho^{m,\varphi(m)}) \leqslant C.$$

By dominated convergence theorem,

$$\lim_{n\to\infty}\int_0^{T_f}\int_{x_1}^{x_2} F(\rho^{m,\varphi(m)})dtdx = \int_0^{T_f}\int_{x_1}^{x_2} F(\rho)dtdx, \tag{16}$$

and $V \in BV([0,T_f];[0,V_{\max}])$ with $\|V\|_{BV([0,T_f];[0,V_{\max}])} \leqslant C$, whence the conclusion. □

Remark 2. Since the solution ρ_V of (1) with $V_d = V$ may contain shocks even if the initial datum is a smooth function, the expression

$$\lim_{\epsilon\to 0}\frac{\rho_{V+\epsilon h}(t,\cdot)-\rho_V(t,\cdot)}{\epsilon} \tag{17}$$

does not define any L^p-function for some $p \in \mathbb{N}$, some admissible perturbations $h \in BV([0,T_f],[0,V_{\max}])$, some initial data ρ_0 and some speed functions V. Thus, a gradient descent algorithm to solve the optimal problem (13) cannot be applied in a general way.

Remark 3. Note that the optimal problem (13) may admit multiple solutions. For instance, if the initial datum $\rho_0 = \rho_{\max}$, then $V \to J(V)$ is a constant function. Therefore, any $V \in BV([0,T_f],[0,V_{\max}])$ such that $\|V\|_{BV} \leqslant C$ is an optimal solution of (13).

4.2 Implementation

We briefly describe the implementation of the control law on the AV to achieve optimal traffic flow using an AV as a moving bottleneck in the traffic stream. The control of traffic using an autonomous vehicle as a moving bottleneck is implemented as an optimization problem, where the speed of the AV is adjusted at each optimal time period. During each time period, the AV travels at the optimal constant speed, unless it is required to drive slower due to local traffic conditions. For a given initial traffic state (density distribution on the roadway) and starting position of the AV, the optimal trajectory is computed that minimizes the total fuel consumption of the entire traffic flow. This optimal AV trajectory consists of a series of speeds to drive at for each successive interval, and is based on the predicted traffic state and corresponding position of the AV as solved using the coupled PDE-ODE system.

For this numerical example, the optimal AV trajectory is found using the genetic algorithm as implemented in the Matlab Global Optimization Toolbox (`ga()`). This is implemented with the objective of minimizing the total fuel consumption as described in Section 4.1. The numerical experiment is conducted over a stretch of highway over the course of one hour.

5. SIMULATION RESULTS

Using the implementation of the numerical method described in Section 3, a numerical example is conducted to demonstrate the ability of a single AV to be controlled to act as a moving bottleneck and reduce the fuel consumption of the overall traffic flow. For the numerical example, we consider the case of a single AV that drives during one hour. The maximum speed of the AV on the roadway is $V_{\max} = 120$ km/h, and the minimum allowable speed of the AV is $V_{\min} = 0$ km/h. The maximum (jam) density on the roadway is considered to be 400 veh/km.

We consider two optimal control approaches for the AV: one in which the AV selects an optimal constant speed for the duration of the experiment, and another in which the AV is allowed to change the speed a set number of times during the experiment. The results of the numerical experiments are described below.

5.1 Optimal constant speed of the AV over one hour

In this example, the AV is considered to drive on a two-lane roadway (i.e., two lanes in the direction of travel of the AV), and thus the AV has influence over one of the two lanes ($\alpha = 0.5$). For any constant initial data $\rho_0 \in [0,\rho_{\max}]$ and $y_0 = 35$, we solve numerically the optimal problem (13) with $T_f = 1$, $V_{\max} = 120$, $x_1 = 30$ and $x_2 = 70$. The optimal solution, denoted by $V_{\text{opt}}(\rho_0)$, is computed using the wave front tracking algorithm presented in Section 3. In Figure 7, we have plotted $V_{\text{opt}}(\rho_0)$ with respect to the initial data ρ_0. Three different optimal driving strategies arise:

- When the initial density ρ_0 is low (between 0 veh/km and 70 veh/km), the use of a moving bottleneck is needed to reduce, in an optimal way, the total fuel consumption.
- When the initial density ρ_0 is moderate (between 70 veh/km and 340 veh/km), the optimal speed of the moving bottleneck is 0 km/h, and thus a fixed bottleneck produces the optimal fuel consumption results when optimizing (13).
- When the initial density ρ_0 is high (between 340 veh/km and 400 veh/km), the number of cars is too large. Therefore, the autonomous vehicles cannot act on the traffic flow. Mathematically speaking, the constraint (1c) is inactive.

In Figure 8, the maximum TFC reduction rate with respect to the initial data ρ_0 is presented. Note that when the density is equal to 176 veh/km, we have a 18.1897% TFC reduction rate leading to a substantial reduction of fuel consumption and causing a real impact on the environment.

5.2 Multiple optimal speeds of the AV over one hour

For this scenario, the AV has influence over one of the three lanes ($\alpha = 0.6$). We allow the AV to adjust the driving speed a total of $N-1$ times during the experiment duration. Therefore, the optimization problem (13) can be rewritten as

$$\inf_{(V,T)\in[0,V_{\max}]^N\times[0,T_f]^{N-1}} J(V^d_{(V,T)}(\cdot)) \tag{18}$$

where the cost function J is defined in (13) and, for every $t \in \mathbb{R}_+$,

$$V^d_{(V,T)}(t) = \sum_{i=1}^{N} V(i)\,\mathbb{1}_{(T(i-1),T(i))}(t),$$

with $T(0) := 0$ and $T(N) = +\infty$.

In Figures 9 and 10, we choose $T_f = 1$, $V_{\max} = 120$, $x_1 = 30$ and $x_2 = 70$ in (13). The initial traffic state is

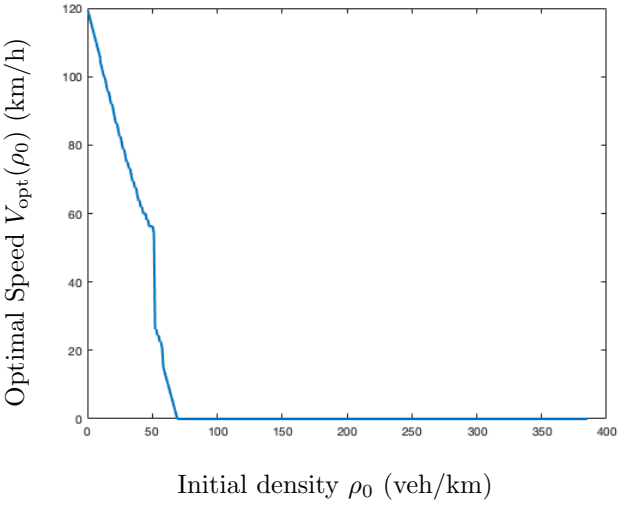

Fig. 7. Plotting of $V_{\text{opt}}(\rho_0)$ with respect to ρ_0.

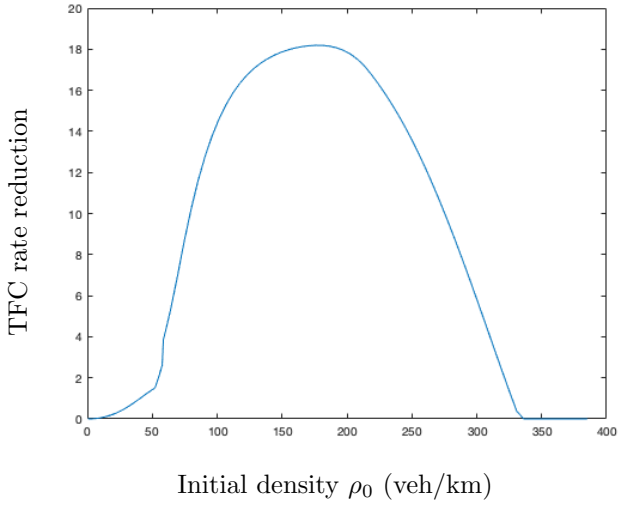

Fig. 8. Plotting of the TFC reduction rate with respect to ρ_0.

$$\rho_0(x) = \begin{cases} 51, & \text{if } x < 50, \\ 270 & \text{if } 50 < x. \end{cases}$$

and $y_0 = 35$. Using the genetic algorithm `ga()`, the optimal maximum speed for for the AV is 38.2 km/h for the first 9.8 minutes, then decrease the speed to 28.3 km/h for the next 4.3 minutes before increasing the speed to 32.7 km/h again for the next 5.2 minutes, 37.2 km/h for the next 6.4 minutes, 56.4 km/h for the next 54.6 minutes and then decreasing again to 27.2 km/h for the final 19.7 minutes in the study time.

As seen in Figure 9, if the AV drives at the maximum possible velocity at all times, the AV encounters the leading edge of the shock wave after roughly 0.2 hours. This results in a total fuel consumption of 16,664 l of fuel. However, when the AV is acting as a moving bottleneck to control the traffic and reduce the fuel consumption, it is able to achieve a lower density gap between the wave

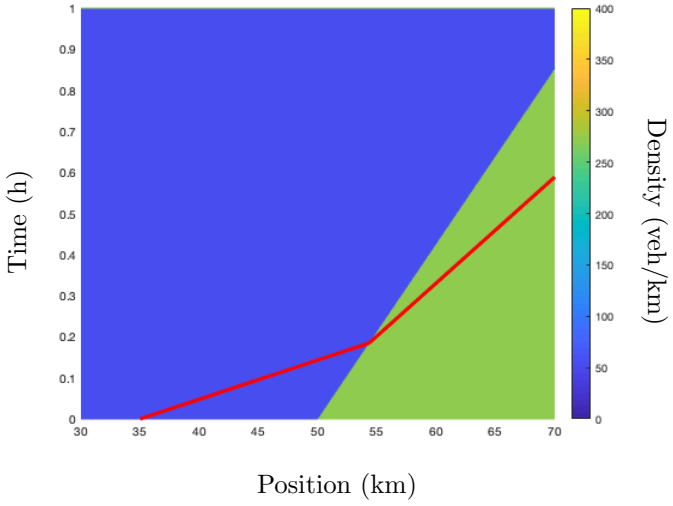

Fig. 9. Traffic density evolution showing wave fronts when the AV drives at the maximum possible speed at all times. The AV trajectory is plotted in red.

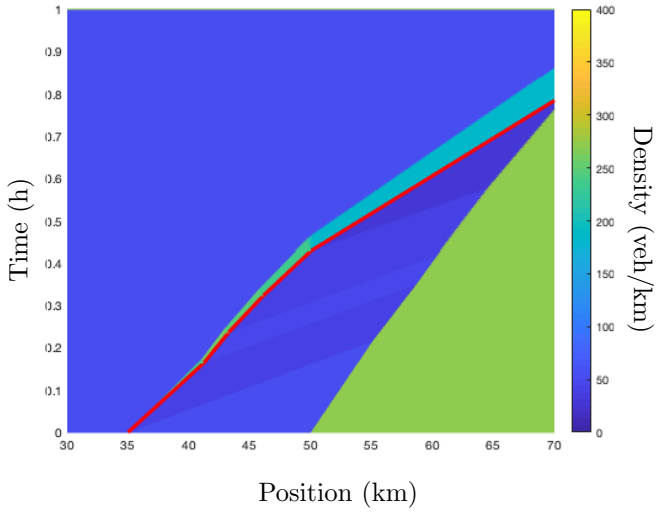

Fig. 10. Traffic density evolution showing wave fronts under the optimal driving strategy. The AV trajectory is plotted in red.

and the AV as seen in Figure 10. By using the control strategy optimized with the genetic algorithm, the total fuel consumption for the same traffic flow is reduced to 16484 l, a reduction of 1.08%.

In Figure 11 and Figure 12, we choose $T_f = 1$, $V_{\max} = 120$, $x_1 = 0$ and $x_2 = 50$ in (13). We consider the case of a single AV that drives in the presence of a fixed bottleneck created at $x = 50$ km; the initial traffic state is

$$\rho_0(x) = \begin{cases} 0, & \text{if } x < -35, \\ 121 & \text{if } 35 < x < 0, \\ 80 & \text{if } 0 < x < 50, \\ 371 & \text{if } 50. \end{cases}$$

and $y_0 = 25$. We have $x_1 = 0$ and $x_2 = 50$.

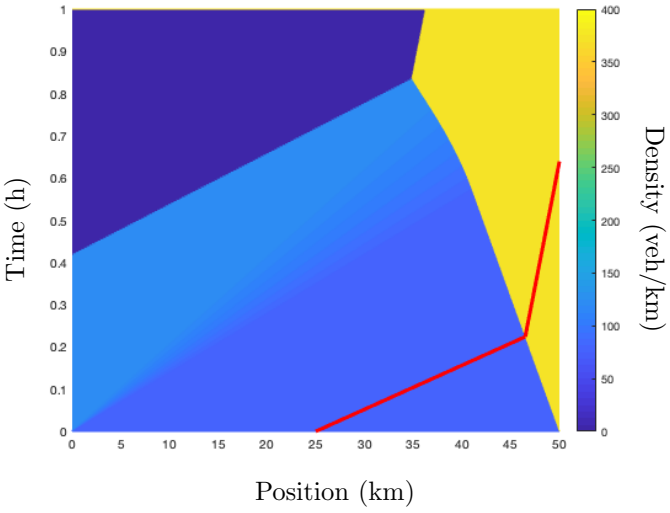

Fig. 11. Traffic density evolution showing wave fronts when the AV drives at the maximum possible speed at all times. The AV trajectory is plotted in red.

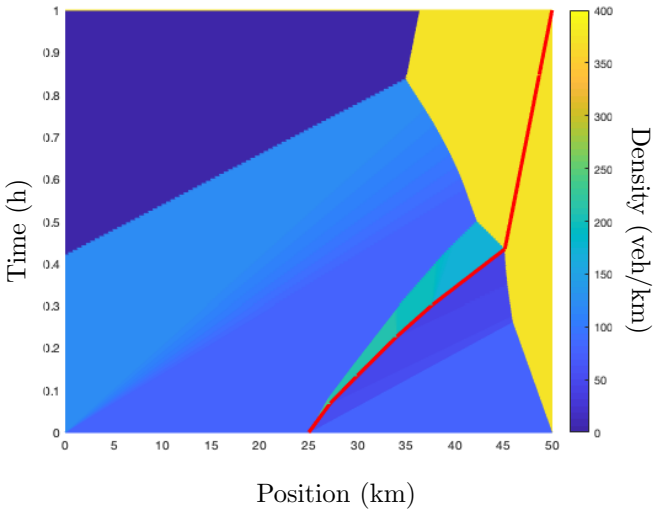

Fig. 12. Traffic density evolution showing wave fronts under the optimal driving strategy. The AV trajectory is plotted in red. Note that the AV reduce its speed smoothly in order to reduce the speed gap when the AV meets the non classical shock created by the fixed bottlenecks.

As seen in Figure 11, if the AV drives at the maximum possible velocity at all times, the AV encounters the leading edge of the shock wave after roughly 0.2 hours. This results in a total fuel consumption of 17740 l of fuel. However, when the AV is acting as a moving bottleneck to control the traffic and reduce the fuel consumption, it is able to achieve a lower density gap between the wave and the AV as seen in Figure 12. By using the control strategy optimized with the genetic algorithm, the total fuel consumption for the same traffic flow is reduced to 17613 l, a reduction of 0.72%.

Figure 10 and Figure 12 indicate that by actively controlling the behavior of the AV to act as a moving bottleneck, it is possible to achieve a reduction in fuel consumption for the entire vehicle fleet, not only the single control vehicle in the flow.

6. CONCLUSIONS

In conclusion, the use of AVs as moving bottlenecks to control traffic flow can be used to reduce total fuel consumption in the presence of a traffic wave.

We have shown that when the AV speed and the initial density are constant, there are three different optimal driving strategies based on the initial density of the traffic. When the density is low, the best driving strategy is obtained using a moving bottleneck. If the density is medium, a fixed bottleneck is more efficient than moving bottlenecks leading to a TFC reduction of 18.1897% when $\rho_0 = 176$ veh/km. As soon as the density is too high, AVs doesn't have any impact on the bulk traffic flow.

When the AV is able to change speeds and adapt to the current traffic conditions, we are able to use the genetic algorithm `ga` to find the optimal AV speed profile throughout the experiment and reduce the total fuel consumption of the bulk traffic flow. The strategy that yielded the best results as shown in Figure 12 is the driving strategy that leads the AV with a smooth speed profile.

7. ACKNOWLEDGMENTS

M. L. Delle Monache was supported by the IDEX-IRS 2018 project "MAVIT". T. Liard was supported by the European Research Council (ERC) under the European Union's Horizon 2020 research and innovation programme (grant agreement NO. 694126-DyCon), by the ELKA-RTEK project KK-2018/00083 ROAD2DC of the Basque Government, by the Grant MTM2017-92996-C2-1-R/2-R COSNET of MINECO (Spain), by the Air Force Office of Scientific Research (AFOSR) under Award NO. FA9550-18-1-0242 and by the grant ICON-ANR-16-ACHN-0014 of the French ANR.

REFERENCES

Ahn, K., Rakha, H., Trani, A., and Van Aerde, M. (2002). Estimating vehicle fuel consumption and emissions based on instantaneous speed and acceleration levels. *Journal of transportation engineering*, 128(2), 182–190.

Berry, I.M. (2010). *The effects of driving style and vehicle performance on the real-world fuel consumption of US light-duty vehicles*. Ph.D. thesis, Massachusetts Institute of Technology.

Čičić, M. and Johansson, K.H. (2018). Traffic regulation via individually controlled automated vehicles: a cell transmission model approach. In *2018 21st International Conference on Intelligent Transportation Systems (ITSC)*, 766–771. IEEE.

Dafermos, C.M. (1972). Polygonal approximations of solutions of the initial value problem for a conservation law. *Journal of Mathematical Analysis and Applications*, 38, 33 – 41.

Delle Monache, M.L. and Goatin, P. (2014). Scalar conservation laws with moving constraints arising in traffic flow modeling: an existence result. *Journal of Differential equations*, 257(11), 4015–4029.

Garavello, M., Goatin, P., Liard, T., and Piccoli, B. (2019). A controlled multiscale model for traffic regulation viaautonomous vehicles. *Preprint*.

Lighthill, M.J. and Whitham, G.B. (1955). On kinematic waves. ii. a theory of traffic flow on long crowded roads. *Proceedings of the Royal Society of London. Series A, Mathematical and Physical Sciences*, 229, 317–345.

Piacentini, G., Goatin, P., and Ferrara, A. (2018). Traffic control via moving bottleneck of coordinated vehicles. *IFAC-PapersOnLine*, 51(9), 13–18.

Ramadan, R.A. and Seibold, B. (2017). Traffic flow control and fuel consumption reduction via moving bottlenecks. *arXiv preprint arXiv:1702.07995*.

Richards, P.I. (1956). Shock waves on the highway. *Operations Research*, 4, 42–51.

Rudin, W. (1976). *Principles of mathematical analysis*. McGraw-Hill Book Co., New York-Auckland-Düsseldorf, third edition. International Series in Pure and Applied Mathematics.

Stern, R.E., Cui, S., Monache, M.L.D., Bhadani, R., Bunting, M., Churchill, M., Hamilton, N., Haulcy, R., Pohlmann, H., Wu, F., Piccoli, B., Seibold, B., Sprinkle, J., and Work, D.B. (2018). Dissipation of stop-and-go waves via control of autonomous vehicles: Field experiments. *Transportation Research Part C: Emerging Technologies*, 89, 205 – 221.